Liquid Crystals
Publication details, including instructions for authors and subscription information:
http://www.informaworld.com/smpp/title~content=t713926090

Achiral bent-core azo compounds: observation of photoinduced effects in an antiferroelectric tilted smectic mesophase

Veena Prasad Corresponding author[a]; Antal Jákli[b]
[a] Centre for Liquid Crystal Research, Bangalore - 560 013, India [b] Liquid Crystal Institute, Kent State University, Kent, OH 44242, USA

To cite this Article Prasad Corresponding author, Veena and Jákli, Antal(2004) 'Achiral bent-core azo compounds: observation of photoinduced effects in an antiferroelectric tilted smectic mesophase', Liquid Crystals, 31: 4, 473 — 479
To link to this Article: DOI: 10.1080/02678290410001660002
URL: http://dx.doi.org/10.1080/02678290410001660002

LIQUID CRYSTALS, VOL. 31, NO. 4, APRIL 2004, 473–479

Taylor & Francis
Taylor & Francis Group

Achiral bent-core azo compounds: observation of photoinduced effects in an antiferroelectric tilted smectic mesophase

VEENA PRASAD*
Centre for Liquid Crystal Research, P.B.No.1329, Jalahalli, Bangalore – 560 013, India

and ANTAL JÁKLI
Liquid Crystal Institute, Kent State University, Kent, OH 44242, USA

(*Received 26 September 2003; accepted 4 December 2003*)

We report the synthesis and physical properties of four novel bent-core compounds, containing an azo linkage and alkyl terminal chains. It is found that, except for the lowest homologue, all the materials are liquid crystalline, exhibiting columnar or tilted polar smectic phases. In one of the compounds a reversible photoinduced variation of the spontaneous polarization of the antiferroelectric state was observed.

1. Introduction

A new surge of activity in the field of ferro-/antiferroelectric liquid crystals has been prompted by the observation of ferroelectric switching in achiral bent-core ('banana-shape') molecules [1]. Following this discovery, a large number of banana-shaped compounds has been synthesized, and at least seven different phases (chronologically assigned as $B_1, \cdots, B_7$) have been described [2–6]. Among them electro-optical switching has been observed only in the smectic B_2, B_5 and B_7 phases. The most widely studied B_2 phase is identified as tilted antiferroelectric polar smectic ($SmCP_A$) phase with either synclinic (SmC_sP_A) or anticlinic (SmC_aP_A) structures [2]. The B_7 phase is unique and interesting due to its beautiful and extraordinary textures [4], and may have a double tilted director structure with C_1 symmetry [7]. The B_1 phase has been designated as a columnar phase with a rectangular lattice [5]. The B_3 and B_4 phases are considered to be crystalline phases [6].

A literature survey reveals that, bent-core molecules containing an azo linkage have not been well studied [8]. The introduction of the $–N=N–$ linkage in such molecules brings a new dimension to this field, namely, photochromism. The first liquid crystalline bent-core azo compounds consisting of six aromatic rings and exhibiting 'banana-smectics' were reported recently [9]. Later several more structural variants of these compounds exhibiting a variety of smectic phases [10] were prepared, but no detailed physical characterization of the materials was carried out, mainly because of their high transition temperatures. In an attempt to reduce the phase transition temperatures we designed and synthesized several new bent-core azo materials consisting of five aromatic rings with three different types of linking groups connecting the aromatic rings to each other to form the bent cores. These compounds exhibited B_1 and B_2 mesophases at fairly low temperatures [11]. It was also noticed that the compounds with alkoxy–alkyl substitution, have lower transition temperatures than the alkoxy–alkoxy substituted compounds.

Based on these observations we have synthesized a new series of bent-core azo compounds with alkyl terminal chains. We find that, although the mesophase ranges are reduced in these new materials, the transition temperatures are even lower than those of the previous materials [11]. In addition, in one of the new compounds we show the first reversible photoinduced variation of the spontaneous polarization.

2. Synthesis

AR quality chemicals and solvents were obtained locally and used without further purification. However, the solvents were dried for use as required. The purity and chemical structures of all the intermediates and the final compounds were confirmed by spectral data. IR spectra were recorded using a Perkin-Elmer 1000 spectrometer. ^1H NMR spectra were recorded in $CDCl_3$ on a 200 MHz Bruker Aveance Series DPX-200 NMR

---

*Author for correspondence; e-mail: veenaclcr@yahoo.com

Liquid Crystals ISSN 0267-8292 print/ISSN 1366-5855 online © 2004 Taylor & Francis Ltd
http://www.tandf.co.uk/journals
DOI: 10.1080/02678290410001660002

spectrometer, using Me_4Si as an internal standard. Microanalyses were performed using a Eurovector Elemental Analyzer, Model Euro EA 3000.

During the synthesis we followed the route reported previously [11] except that we have alkyl substitution at both ends of the molecule (see the scheme). Accordingly, 4-hydroxybenzaldehyde was esterified with 4-*n*-octylbenzoic acid to obtain aldehyde **1**. This was reacted with 3-aminobenzoic acid in ethyl alcohol under reflux, to obtain acid **2**. Finally, acid **2** was esterified with the required 4-*n*-alkyl-4′-hydroxyazobenzenes [12], in the presence of 1,3-dicyclohexylcarbodiimide and DMAP as a catalyst, using dry dichloromethane as solvent. The alkyl chain *R* at one end was fixed as C_8H_{17}. The chain length at the other end *R*′ was systematically varied from C_6H_{13} to $C_{12}H_{25}$ (**AB6–AB12**). The final materials were purified by several recrystallizations using butan-2-one as solvent. The spectral data and microanalyses obtained for all the compounds were satisfactory. The analytical data obtained for **AB12** are: IR ν_{max} cm^{-1} (KBr pellet): 2927, 2849, 1731, 1626, 1596, 1576, 1499, 1262, 1229, 1200, 1162, 1179, 1078, 923, 866. ^1H NMR ($CDCl_3$) δ: 8.55 (s, 1H, –CH–N–), 7.31–8.14 (m, 20H, ArH), 2.65–2.74 (m, 4H, Ar–CH_2), 1.26–1.75 (m, 32H, –CH_2–), 0.88 (m, 6H, –CH_3). Elemental anal: calcd for $C_{53}H_{63}N_3O_4$, C 78.97, H 7.88, N 5.21; found, C 78.99, H 7.82, N 5.29 %.

3. Physical properties

The transition temperatures and associated enthalpies were determined by differential scanning calorimetry (DSC7, Perkin-Elmer) at heating and cooling rates of 5°C min^{-1}. All the compounds were found to be thermally stable. The transition temperatures and associated enthalpy changes are given in the table. As expected, the transition temperatures and the thermal stability of the mesophases are lower than those of the alkoxy–alkoxy and alkoxy–alkyl substituted compounds [11]. In addition we find that the melting points as well as the clearing temperatures decrease

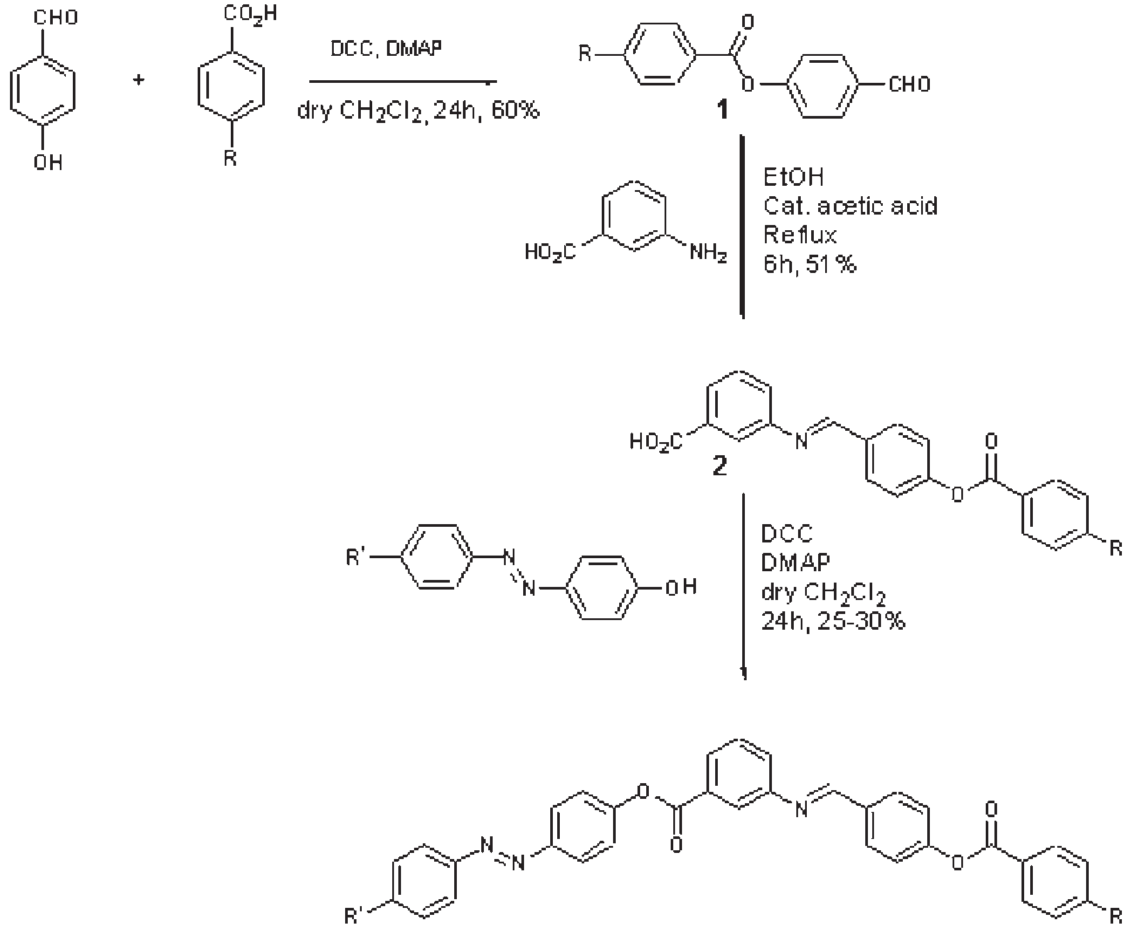

AB6 –AB12

Scheme. Synthetic scheme used to obtain the **AB6–AB12** series.

Table 1. Transition temperatures and associated enthalpy changes for the series **AB6**–**AB12**.

Compound	*R*	*R′*	Phase sequence in °C (enthalpies in kJ mol^{-1})
AB6	C_8H_{17}	C_6H_{13}	$\mathrm{I} \underset{138.9(23.1)}{\overset{131.5(26.7)}{\rightleftarrows}} \mathrm{Cr}$
AB8	C_8H_{17}	C_8H_{17}	$\mathrm{I} \overset{\xrightarrow{132.9(17.2)} \mathrm{Col} \xrightarrow{120.3(18.8)}}{\xleftarrow[134.6(38.1)]{\hspace{6em}}} \mathrm{Cr}$
AB10	C_8H_{17}	$C_{10}H_{21}$	$\mathrm{I} \underset{132.3(17.3)}{\overset{131.0(17.7)}{\rightleftarrows}} \mathrm{SmC_sP_A} \underset{128.4(0.2)}{\overset{127.9(0.22)}{\rightleftarrows}} \mathrm{SmC_aP_A} \underset{126.9(19.8)}{\overset{110.0(16.7)}{\rightleftarrows}} \mathrm{Cr}$
AB12	C_8H_{17}	$C_{12}H_{25}$	$\mathrm{I} \underset{131.1(18.6)}{\overset{129.6(18.5)}{\rightleftarrows}} \mathrm{SmC_aP_A} \underset{120.5(35.1)}{\overset{110.9(19.4)}{\rightleftarrows}} \mathrm{Cr}$

with increasing chain length. The compound **AB6** ($R' = C_6H_{13}$) is not mesomorphic; **AB8** ($R' = C_8H_{17}$) shows only a monotropic mesophase; **AB10** ($R' = C_{10}H_{25}$) exhibits two enantiotropic mesophases separated by a weak first-order transition, while **AB12** ($R' = C_{12}H_{25}$) has an single enantiotropic mesophase.

The microscopic structures of the enantiotropic mesophases (for **AB10** and **AB12**) were determined by X-ray measurements carried out in the Midwest Universities Collaborative Access Team (MUCAT) Powder Diffraction station of the Advanced Photon Source of the Argonne National Laboratory ($E = 9.684$ keV, $\lambda = 1.2803$Å, 3450×3450 resolution, detector at 378.499 mm from the sample). The measurements reveal a single small angle diffraction peak at $2\theta = 1.9$ (2.0) degrees corresponding to a ~ 38.6 Å (37.2 Å) layer spacing for **AB10** (**AB12**). These distances are clearly smaller than the end-to-end distances (~ 50 Å) of the bent-core molecules indicating tilted smectic phases with about a 35°–40° tilt angle. At wide angles only a single diffuse peak is seen, implying fluid in-plane structures. The small angle peaks are shown in figures 1 (*a*) and 1 (*b*) for materials **AB10** and **AB12**, respectively.

Polarizing microscopy and polarization current measurements were carried out in 4 µm films after filling the materials into cells obtained from Displaytech. The liquid crystal cells were placed in a computer-controlled heating stage (STC2000F from Instec Inc.) and the textures were studied using a polarizing microscope (BX 60 from Olympus). For electric current measurements and electro-optical studies a digital oscilloscope (HP 54600B), a digital multimeter (HP 34401A) and an arbitrary waveform generator (HP 33120A) were used. The time dependences of the electric current flowing through the samples were

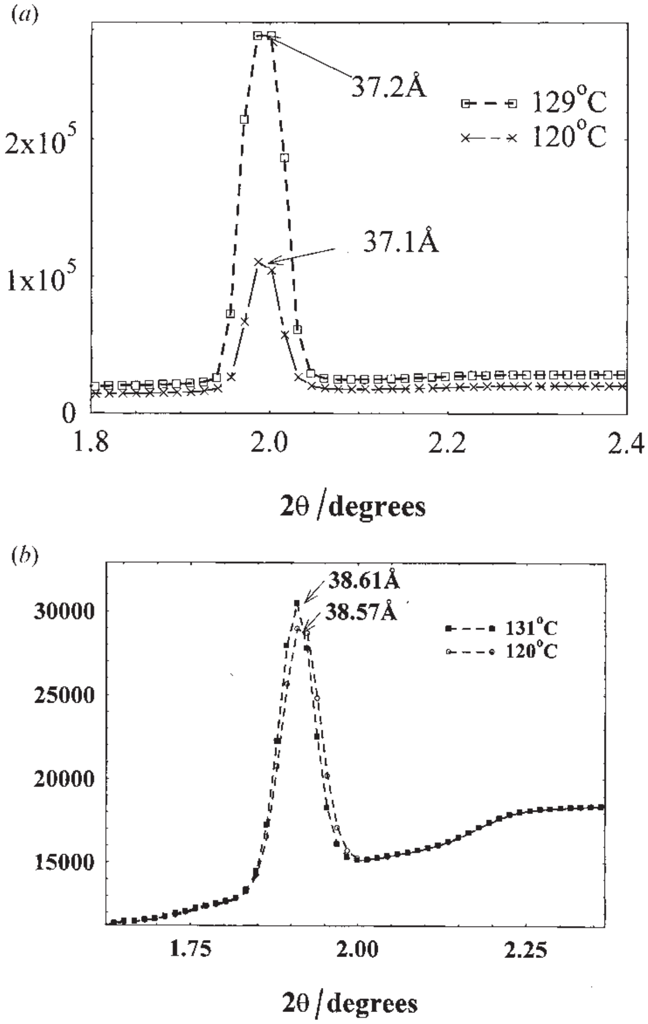

Figure 1. Small-angle X-ray diffraction results on 16 µm thick films of (*a*) **AB10** and (*b*) **AB12** at the high and low temperature ranges of the enantiotropic mesophases.

measured both under triangular and rectangular voltage excitations. The time dependence of the polarization current under triangular waveforms gives the nature of the polar phase (antiferroelectric or ferroelectric), and the magnitude of the polarization involved in the switching; whereas from the peak position of the polarization current under rectangular waveforms we can deduce the switching time.

The monotropic mesophase of material **AB8** grows in the form of dendritic domains on cooling from the isotropic phase indicating a columnar (B_1) mesophase. The structure could not be switched using fields up to 40 V μm^{-1} Typical textures during and below the clearing point are shown in the top row of figure 2.

For **AB10** the weak first order transition at 128°C seen by DSC is not clearly visible in the polarization current measurements. The polarization switching is antiferroelectric in both ranges; furthermore the magnitude of the polarization and the switching times increase monotonously with no noticeable change at 128°C (see figure 3). The only difference to be seen is that the switching angle drops to zero at 128°C, then remains at zero up to the clearing point. Combining this observation with the X-ray results (that show only minor temperature dependence of the layer spacing), we conclude that both are antiferroelectric tilted smectic phases, with the higher temperature range being racemic (SmC_sP_A), whereas the lower temperature range is chiral (SmC_aP_A). The textures in the chiral antiferroelectric SmC_aP_A phase are shown in the middle

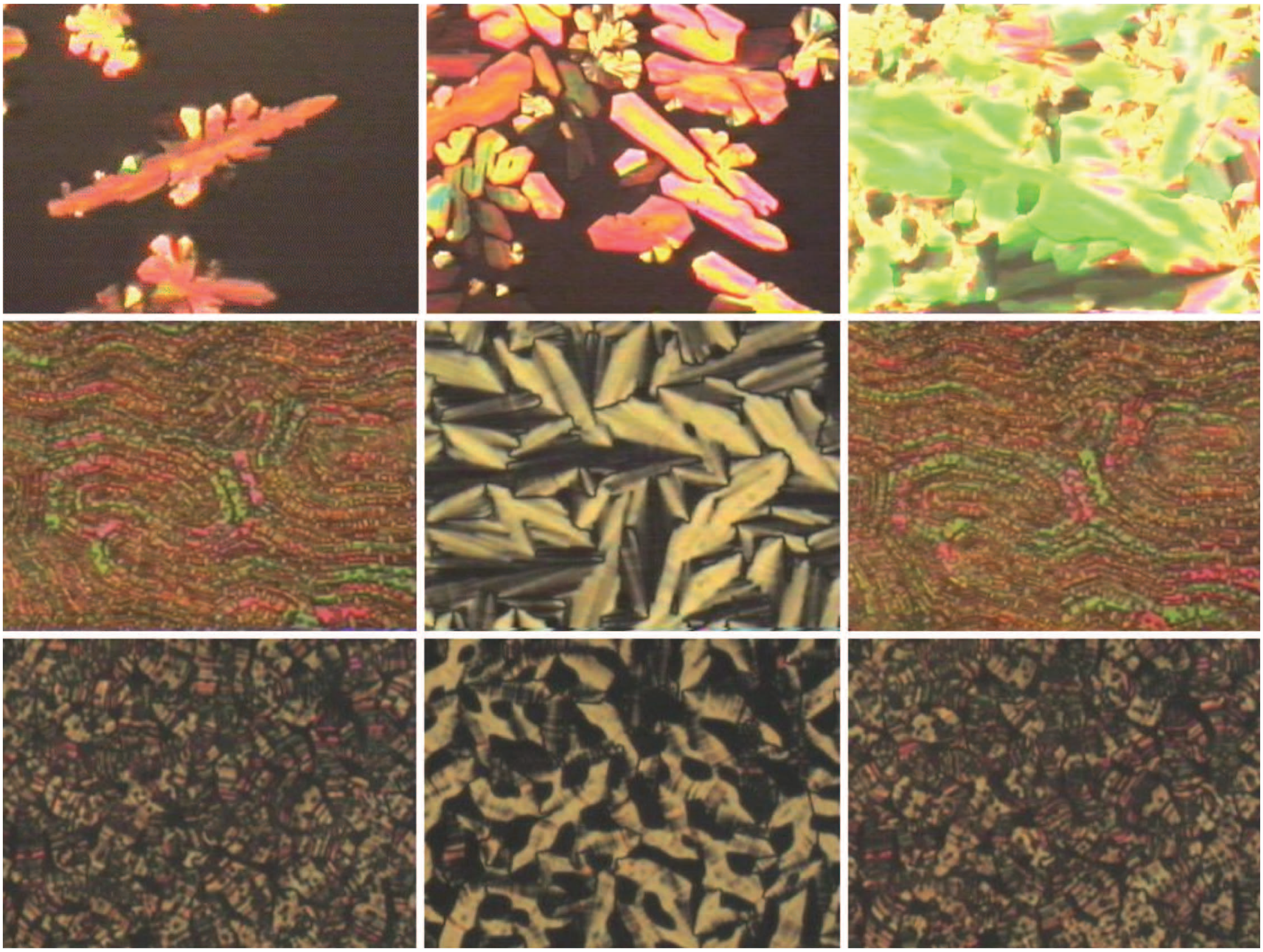

Figure 2. Polarizing microscopic textures of the compounds **AB8–AB12**. Top row: **AB8** (left and middle) at 129°C under cooling; (right) at 125°C. Pictures represent about $130\times100\,\mu m^2$ areas. Middle row: **AB10** (left) $E=-15\,V\,\mu m^{-1}$; (middle) $E=0$; (right) at $E=+15\,V\,\mu m^{-1}$ fields. In the left and right pictures a $\lambda/4$ plate is inserted to emphasize the differences in opposite fields. Pictures represent $133\times100\,\mu m^2$ areas; temperature 125°C. Bottom row: **AB12** (left) $E=-12.5\,V\,\mu m^{-1}$; (middle) at $E=0\,V\,\mu m^{-1}$; (right) $E=+12.5\,V\,\mu m^{-1}$. Pictures represent $133\times100\,\mu m^2$ areas; temperature 125°C.

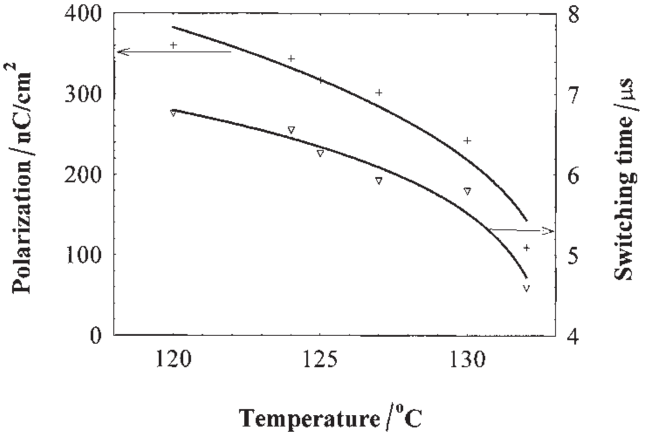

Figure 3. Temperature dependences of the ferroelectric polarization and switching time measured under 13 V μm^{-1} fields for **AB10**.

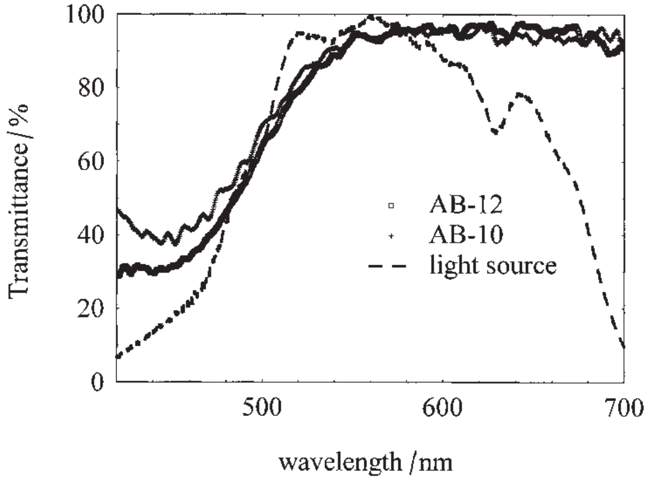

Figure 4. Normalized light intensity spectrum of the halogen microscope lamp (HLX 64623 from Osram) and the transmittance of **AB10** and **AB12** at $T = 125$°C.

row of figure 2 both in the antiferroelectric and in the field-induced ferroelectric states. We observed that the clearing point of **AB10** is suppressed by about 1°C when illuminated by the light of a 100 W halogen lamp in the polarizing microscope. Apart from this, no observable change in the magnitude of the polarization or in the switching processes was detected.

For **AB12** there is only one switchable polar smectic phase, in agreement with DSC observations. As with **AB10**, the polarization reversal current shows two peaks in each half period of the triangular waveform of the applied electric field, indicating that the phase is antiferroelectric. Depending on the polarity of the electric field the optic axis rotates back and forth indicating a chiral ($\mathrm{SmC_aP_A}$) structure. In this material we could not detect the racemic texture independent of the history of the sample. Typical textures in the antiferroelectric state and in the field-induced ferroelectric states are shown in the bottom row of figure 2.

It was observed that the value of the polarization, the switching threshold, the switching times and the electric conductivity values depend on the light illumination during measurements. The material was illuminated by a 100 W halogen photo optic lamp (Xenophot, HLX 64623). Its normalized spectrum together with the transmittance of the **AB10** and **AB12** samples are shown in figure 4. It can be seen that both **AB10** and **AB12** absorb light strongly in the blue region, with the difference that the absorption of **AB12** is somewhat stronger, especially in the low wavelength region. In spite of this relatively small difference, the electric polarization reduction was observed only for **AB12**. Specifically, for **AB12** at 0.15 W cm^{-2} light intensity the electric polarization values decrease by about 20%, the threshold field for switching from the antiferroelectric to the ferroelectric states decrease by 0.35 V μm^{-1}, and the switching times increase by about 0.3 μs in the whole $\mathrm{SmC_aP_A}$ range. The intensity dependence of the variation of the spontaneous polarization is illustrated in figure 5 (*a*). The data were fitted using the equation:

$$\Delta P = \Delta P_{\max} \Big/ \left[1 + \left(\frac{I_o}{I}\right)^2\right]$$

with parameters $\Delta P_{\max} = -31.5\,\mathrm{nC\,cm^{-2}}$ and $I_o = 0.14\,\mathrm{W\,cm^{-2}}$. The variations of the physical parameters are reversible with relaxation and onset times in the range 5–10 s. The time dependence of the electric polarization under illuminated and dark conditions are shown in figure 5 (*b*). The temperature dependences of the amplitude of the ferroelectric polarization values and the switching times, measured both in the dark and during illumination by microscope light, are shown in figures 6 (*a*) and 6 (*b*), respectively. The clearing point under illumination (130.1°C) is 0.9°C lower than in the dark; however this difference cannot account for the noted differences in the physical parameters.

4. Discussion

The decrease of the ferroelectric polarization is most likely due to a photochemical isomerization processes. In the molecules studied there are two connecting groups that are sensitive to light: the azo group and the azomethine unit. However, we rule out the possibility of photoisomerisation of the azomethine unit under the experimental conditions used in the present studies. Therefore we propose that only the azo linkage undergoes *trans–cis* isomerization. Since the azo unit is incorporated only on one side of the molecules, this isomerization leads to a zigzag shape. We note that,

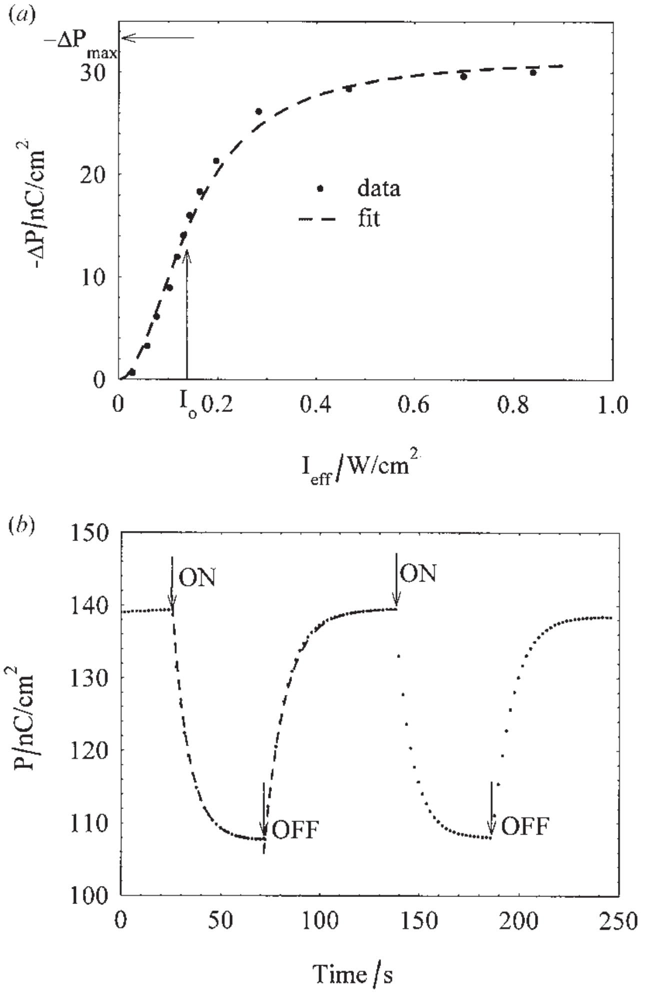

Figure 5. (*a*) Variation of the spontaneous polarization as a function of the effective light intensity for **AB12** at $T = 125^{\circ}\mathrm{C}$. (*b*) Time dependence of the electric polarization under the application of the $0.14\,\mathrm{W\,cm^{-2}}$ light and on turning it off.

even without taking into account a possible photo-induced decrease of the polar order, photoisomerisation leads to a decrease of the ferroelectric polarization, since in the zigzag shape the contributions of molecular dipoles in the arm containing the azo linkage partially cancel each other. We note that the absorption induced heating effect is less than 0.5°C from the measurement of the steady values of the resistance in the dark and bright states. This and the light-induced disordering together cause the observed 0.9°C suppression of the clearing point, which results in only a small contribution to the observed change of the polarization. We note that a light-induced polarization decrease is known for azo dye-doped ferroelectric SmC* liquid crystals [13–16], but there the effect is mainly due to light-induced disordering leading to more than a 10°C

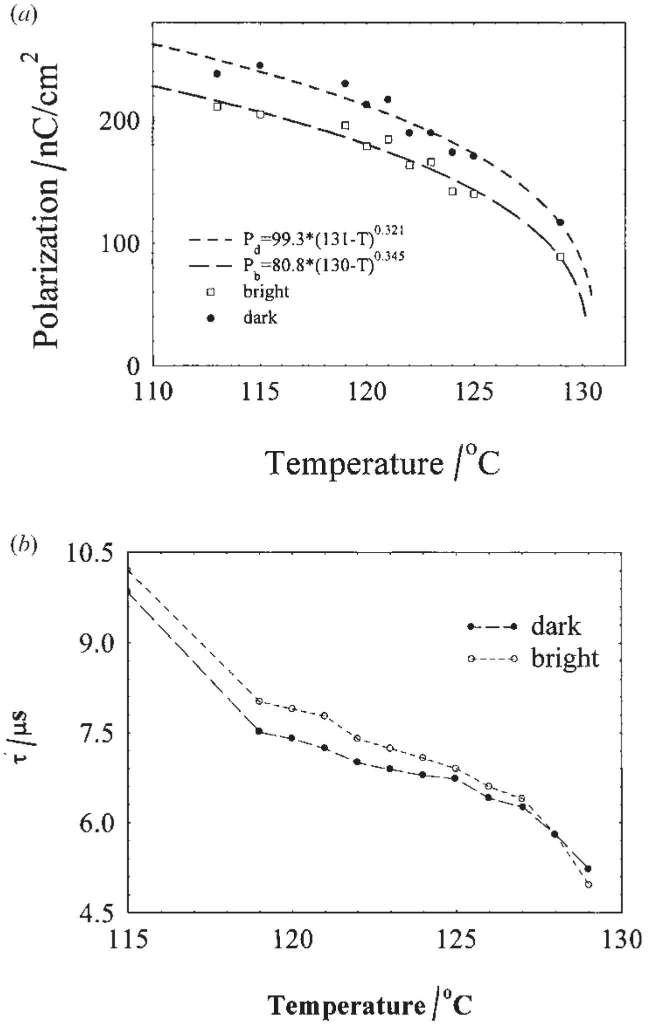

Figure 6. Temperature dependences of (*a*) the polarization and (*b*) the switching time as measured under a $13\,\mathrm{V\,\mu m^{-1}}$ field in dark and illuminated environments for **AB12**. The illumination is provided by a 100 W halogen photo-optic lamp (Xenophot, HLX 64623) of the polarizing microscope Olympus BX60.

suppression of the clearing point. The physical mechanism of the reversible light-induced changes observed here is different therefore from that seen in these previous studies. More detailed optical and electrical studies are in progress [17] to verify this model and to clarify why we could not see similar effects for **AB10**, which has a very similar phase sequence and molecular structure.

The Midwest Universities Collaborative Access Team (MUCAT) sector at the APS is supported by the U.S. Department of Energy, Office of Science, Office of Basic Energy Sciences, through the Ames Laboratory under Contract No. W-7405-Eng-82. We are grateful to

Professor Satyendra Kumar for useful discussions about X-ray measurements.

References

[1] Niori, T., Sekine, T., Watanabe, J., Furukawa, T., and Takezoe, H., 1996, *J. mater. Chem*, **6,** 1231.

[2] Link, D. R., Natale, G., Shao, R., Maclennan, J. E., Clark, N. A., Korblova, E., and Walba, D. M., 1997, *Science*, **278,** 1924.

[3] Walba, D. M., Korblova, E., Shao, R., Maclennan, J. E., Link, D. R., Glaser, M. R., and Clark, N. A., 2000, *Science*, **288,** 2181; Rouillon, J. C., Marcerou, J. P., Laguerre, M., Nguyen H. T., and Achard, M. F., 2001, *J. mater. Chem*., **11,** 2946.

[4] Pelzl, G., Diele, S., Jákli, A., Lischka, CH., Wirth, I., and Weissflog, W., 1999, *Liq. Cryst.*, **26,** 135.

[5] Shen, D., Pegenau, A., Diele, S., Wirth, I., and Tschierske, C., 2000, *J. Am. chem., Soc.*, **122,** 1593.

[6] Pelzl, G., Diele, S., and Weissflog, W., 1999, *Adv. Mater.*, **11,** 707 and references therein.

[7] Jákli, A., Krüerke, D., Sawade, H., and Heppke, G., 2001, *Phys. Rev. Lett.*, **86,** 5715.

[8] Prasad, V., 2001, *Liq. Cryst.*, **28,** 145.

[9] Prasad, V., Rao, D. S. S., and Prasad, S. K., 2001, *Liq. Cryst.*, **28,** 643.

[10] Prasad, V., 2001, *Mol. Cryst. liq. Cryst.*, **363,** 167.

[11] Prasad, V., Kang, S.-W., and Kumar, S., 2003, *J. mater. Chem.*, **13,** 1259.

[12] Ikeda, T., Miyamoto, T., Kurihara, S., Tsukada, M, and Tazuke, S., 1990, *Mol. Cryst. liq. Cryst.*, **182B,** 357.

[13] Ikeda, T., Sasaki, T., and Ichimura, K., 1993, *Nature* **361,** 428; Sasaki, T., and Ikeda, T., 1993, *Ferroelectrics*, **149,** 343; Sasaki, T., Ikeda, T., and Ichimura, K., 1994, *J. Am. chem. Soc.*, **116,** 625; Sasaki, T., and Ikeda, T., 1995, *J. phys. Chem*, **99,** 13002; Sasaki, T., and Ikeda, T., 1995, *J phys. Chem*, **99**, 13013.

[14] Coles, H. J., Walton, H. G., Guillon, D., and Poetti, G., 1993, *Liq. Cryst.*, **15,** 551; Walton, H. G., Coles H. J., Guillon D., and Poetti, G., 1994, *Liq. Cryst.*, **17,** 333.

[15] Blinov, L. M., Kozlowsky, M. V., Ozaki, M., and Yoshino, K., 1996, *Mol. Mater.*, **6,** 235; Blinov, L. M., Kozlowsky, M. V., Nakayama, K., Ozaki, M., and Yoshino, K., 1996, *Jpn. J. appl. Phys*., **35,** 5405; Demikhov, E. I., John, M., and Krohn, K., 1997, *Liq. Cryst*., **23,** 443.

[16] Öge, T., and Zentel, R., 1996, *Macromol. Chem. Phys.* **197,** 1805; Fischer, B., Thieme, C., Fischer, T. M., Kremer, F., Öge, T., and Zentel, R., 1998, *Polym. adv. Tech*., **9,** 665; Langhoff, A., and Giesselmann, F., 2000, *Ferroelectrics*, **244,** 283.

[17] Jákli, A., Prasad, V., Rao, D. S. S., and Jánossy, I. (to be published.).